

Fixed bed adsorption of chromium and the Weibull function

Khim Hoong Chu

Honeychem Research, Auckland 1142, New Zealand



ARTICLE INFO

Keywords:

Asymmetric breakthrough curve
Bohart-Adams
Fixed bed adsorption
Probability distribution
Weibull function

ABSTRACT

Fixed bed adsorption of toxic metal ions such as chromium is a research area of current interest. Mathematical models are routinely used to summarize breakthrough results of metal ions, which often display varying degrees of curve asymmetry. This work introduces the Weibull function as a simple model for correlating asymmetric breakthrough curves of chromium. The Weibull function is similar to the widely used Bohart-Adams model in several aspects. For example, they both produce sigmoid or S-shaped curves. Their simple mathematical forms can be linearized and linear regression can then be used to estimate their parameters. However, the Weibull function, unlike the Bohart-Adams model, can track the trajectory of asymmetric breakthrough data. Applying the Weibull function to published breakthrough data of chromium, this article illustrates its outright superiority versus the Bohart-Adams model in representing highly asymmetric data. Both equations provide satisfactory fits to breakthrough data exhibiting a moderate degree of curve asymmetry.

1. Introduction

Certain types of industrial wastewaters contain toxic metal ions. Chromium is a typical example commonly found in electroplating wastewater (GracePavithra et al., 2019). Although a variety of methods have been proposed for chromium removal from aqueous solutions (Peng and Guo, 2020), adsorption is considered a highly efficient treatment method, especially for processing waste streams contaminated by trace quantities of chromium. Many commercial and natural adsorbents have been tested for their effectiveness in removing chromium from synthetic solutions and, on occasion, from actual industrial wastewater. The adsorption process in wastewater decontamination usually involves fixed bed columns. A proven design approach for sizing fixed bed columns is the so-called bed depth-service time (BDST) method (Hutchins, 1973), which uses pilot test data to calibrate the BDST design equation. This design approach has worked fairly well since its introduction in the 1970's because it only requires information from the initial parts of breakthrough curves where the breakthrough or service times reside. As is well known, the BDST equation is a rearranged form of the widely used Bohart-Adams model of fixed bed adsorption (Bohart and Adams, 1920).

In cases where one wishes to use a model to capture the breakthrough and exhaustion times of an observed breakthrough curve, it becomes necessary to fit the model to the entire breakthrough profile. Experiments conducted with laboratory and pilot fixed bed columns often lead to tailing breakthrough curves. This curve asymmetry is typically observed when the effluent concentration approaches the influent concentration slowly near column saturation. The BDST/Bohart-Adams model is not

expected to provide a good fit to asymmetric breakthrough curves because its mathematical form is by design symmetric (Oulman, 1980). A breakthrough curve exhibiting strong tailing tends to make the Bohart-Adams model fit poorly to both its initial and saturation parts, resulting in unreliable estimates of breakthrough and exhaustion times. There is however a shortage of mathematical models capable of handling breakthrough curve asymmetry. So far, only a handful of studies have proposed such models, as summarized by Apiratikul and Chu (2021).

Because typical breakthrough curves resemble probability cumulative distributions, some studies have used probability functions to model sigmoid breakthrough curves. For example, a fixed bed model based on the normal or Gaussian probability distribution for fitting chromium breakthrough curves has been presented by Dima et al. (2020). The Gompertz probability distribution has been applied to the modeling of chromium, copper, and methylene blue breakthrough curves (Chu, 2020a). This paper highlights the potential of the Weibull probability distribution (Weibull, 1951) as a model for correlating asymmetric breakthrough curves of chromium.

Use of the Weibull function to represent curve shapes in a variety of scientific disciplines is widespread. In the area of adsorption, the Weibull probability density function has been used to derive the Dubinin-Astakhov adsorption isotherm (Chen and Yang, 1994; Hutson and Yang, 1997). The Weibull cumulative distribution function has been used as an isotherm model as well as a batch kinetic model to fit respectively the equilibrium data (Altenor et al., 2009; Ncibi et al., 2008; Njoku et al., 2015) and kinetic data (Guiza et al., 2021; Selmi et al., 2018) of several water contaminants. Interestingly, the Weibull function is analogous to the Avrami equation

E-mail address: khimchu@gmail.com (K.H. Chu).

<http://doi.org/10.1016/j.hazl.2021.100022>

Received 30 December 2020; Received in revised form 9 March 2021; Accepted 24 March 2021

Available online 27 March 2021

2666-9110/© 2021 The Author(s). Published by Elsevier B.V. This is an open access article under the CC BY-NC-ND license (<http://creativecommons.org/licenses/by-nc-nd/4.0/>)

(Avrami, 1940), which is used to describe the kinetics of phase change with emphasis on crystal growth (Marangoni, 1998). A review on the modeling of batch adsorption kinetics of water contaminants using the Weibull-Avrami equation has been given by Oladoja (2016).

So far as the author knows, little is known regarding the ability of the Weibull function to describe breakthrough curves of water contaminants. To address this research gap, the data fitting ability of the Weibull function is tested in this study using chromium breakthrough data collated from previous reports published in the *Journal of Hazardous Materials*. Its performance is compared to that of the Bohart-Adams model. It should be noted that the Bohart-Adams model is analogous to the Thomas and Yoon-Nelson models (Chatterjee and Schiewer, 2011; Lee et al., 2015). So, it makes no difference which of the three models is used, as the results will be identical.

2. Fixed bed models

2.1. Weibull function

The Weibull cumulative distribution function, formulated for adsorption, may be written

$$\frac{c}{c_0} = 1 - \exp \left[- \left(\frac{t}{a} \right)^b \right] \quad (1)$$

where c is the effluent concentration at any time t , c_0 is the feed concentration, $a > 0$ is a rate parameter, and $b > 0$ is a shape parameter. The Weibull function generates S-shaped curves for $b > 1$. Its two unknown parameters, a and b , can be easily determined using a spreadsheet program with a built-in optimization routine. Because the two parameters lack physical significance, their values are usually extracted from breakthrough data. It is not possible to determine the two parameters from independent sources (e.g., engineering correlations).

The Weibull function can be transformed into linear form and linear regression can then be used to estimate its parameters. One version of the linearizing transformation is given by

$$\ln \left[-\ln \left(1 - \frac{c}{c_0} \right) \right] = b \ln(t) - b \ln(a) \quad (2)$$

If this equation is obeyed, plots of its left-hand member against $\ln(t)$ should give a straight line. However, fitting the linearized Weibull function to breakthrough data by linear regression to estimate its parameters is a procedure fraught with statistical problems.

2.2. Bohart-Adams model

A simplified version of this century-old model is written as

$$\frac{c}{c_0} = \frac{1}{1 + \exp(\alpha - \beta t)} \quad (3)$$

where

$$\alpha = \frac{k_{BA} N_0 L}{u} \quad (4)$$

$$\beta = k_{BA} c_0 \quad (5)$$

In Eqs. (4) and (5), k_{BA} is the Bohart-Adams rate coefficient, N_0 is the amount of contaminant adsorbed per unit volume of fixed bed, L is the bed depth, and u is the superficial velocity. The two parameters to be estimated are α and β (or k_{BA} and N_0). The Bohart-Adams model can be treated as a probability distribution because its functional form resembles the cumulative distribution of the logistic function.

3. Nonlinear least-squares regression

The unknown parameters of the Weibull and Bohart-Adams models were estimated using nonlinear least-squares regression. Overall fit was assessed using the residual root mean square error (RRMSE) (Kinniburgh, 1986) given by

$$\text{RRMSE} = \sqrt{\frac{\sum_{j=1}^n (E_j - M_j)^2}{n - p}} \quad (6)$$

where E_j are experimental values of c/c_0 , M_j are model values of c/c_0 , n is the number of data points, and p is the number of adjustable parameters. A lower RRMSE value indicates a better fit.

4. Results and discussion

In this work, three sets of published breakthrough data of chromium are used to test the Weibull function: (1) Cr(III) adsorption by olive stone particles reported by Calero et al. (2009), (2) Cr(III) removal by a biosorbent reported by Romero-González et al. (2009), and (3) Cr(VI) adsorption by coir pith particles reported by Suksabye et al. (2008).

4.1. Case 1: Cr(III) adsorption by olive stone particles

This example deals with Cr(III) adsorption by olive stone particles which were packed in a glass column with an internal diameter of 1.5 cm and a total column length of 23 cm (Calero et al., 2009). The olive stone adsorbent was obtained by milling raw olive stones with an analytical mill and choosing a fraction lower than 1 mm. A series of breakthrough curves were generated by varying the feed flow rate, inlet concentration, and packed bed length. The pH and temperature were maintained at pH 4 and 25 °C, respectively. One set of breakthrough data, obtained with the following conditions: $c_0 = 10 \text{ mg/L}$, $L = 13.4 \text{ cm}$, and $u = 1.13 \text{ cm/min}$, is shown in Fig. 1.

With a relatively large empty bed contact time of approximately 12 min, it is somewhat surprising to observe that Cr(III) emerged fairly

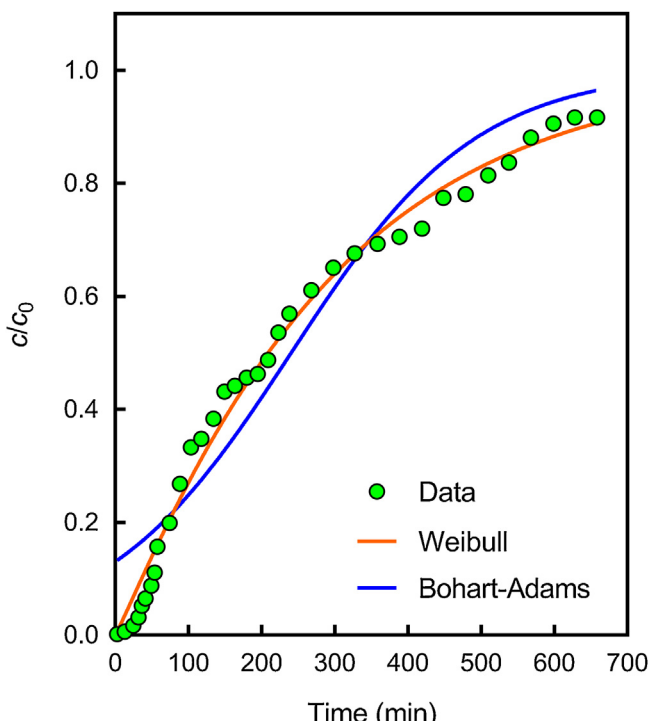


Fig. 1. Bohart-Adams and Weibull fits compared to observed Cr(III) breakthrough data reported by Calero et al. (2009).

quickly at the column outlet. The olive stone adsorbent was most likely non-porous, offering a limited external surface area for adsorption. As a result, its uptake capacity for Cr(III) was rather poor, which led to the early breakthrough seen in [Fig. 1](#).

As [Fig. 1](#) shows, the observed breakthrough curve is highly asymmetric—an initial, rapid rise in the effluent concentration, followed by a gradual approach to column saturation. [Fig. 1](#) plots the Bohart-Adams and Weibull fits. The resultant parameter estimates and fit statistics are provided in [Table 1](#), case 1. [Fig. 1](#) shows that the Bohart-Adams fit is a complete failure, bypassing most of the data points. The Weibull fit, by contrast, is very effective, tracking closely most of the data points and reproducing the overall shape of the experimental profile. As [Table 1](#) shows, the RRMSE values for the two fits make it apparent that the Weibull function is the superior fit.

The superiority of the Weibull function versus the Bohart-Adams model is to a large extent due to the fact that the former has a floating inflection point while the latter has a fixed one. Every sigmoid breakthrough curve has an inflection point. A breakthrough curve is said to be symmetric if its inflection point is located at $c/c_0 = 0.5$, that is, the mid-point of the curve. It follows that an inflection point located at other c/c_0 values indicates an asymmetric breakthrough curve. The inflection point of a sigmoid breakthrough curve can be estimated in two simple steps. First, the time value at the inflection point is estimated by equating the second derivative of the model equation to zero and solving the resulting equation for the t -term. Second, plugging the estimated time value into the model equation yields the c/c_0 value corresponding to the inflection point.

The inflection point of the Bohart-Adams model is well known. As pointed out by [Oulman \(1980\)](#), the Bohart-Adams model and the logistic equation are fully equivalent. It is a widely known fact that the inflection point of the logistic equation is located at the mid-point. It follows that the inflection point of the Bohart-Adams model is located at $c/c_0 = 0.5$. This invariant inflection point confines the Bohart-Adams model to producing perfectly symmetric breakthrough curves regardless of the values of its two parameters. This is the reason why it failed to track the highly asymmetric breakthrough data depicted in [Fig. 1](#). Fitting the Bohart-Adams model to such data is doomed to failure.

The inflection point of the Weibull function is not so well known; it can of course be derived by applying the procedure outlined above to Eq. (1). The result is

$$\frac{c}{c_0} = 1 - \exp\left(-\frac{b-1}{b}\right) \quad (7)$$

The last result indicates that the inflection point of the Weibull function varies with the b -term. So, the Weibull function has a floating or variable inflection point. Note that the Weibull function generates sigmoid curves if $b > 1$. For $b \leq 1$, Eq. (7) breaks down and no inflection point exists. Consequently, the Weibull function produces hyperbolic curves instead of sigmoid ones. This explains why the Weibull function can be used to fit hyperbolic trends of adsorption equilibrium data as well as batch kinetic data, as mentioned in the Introduction. If the b -term is close to unity, the inflection point is located close to the origin. If the b -term is very large, Eq. (7) becomes $c/c_0 = 1 - \exp(-1) = 0.632$, which represents the upper limit for the location of the inflection point.

Table 1

Parameter estimates and RRMSE values for the Bohart-Adams and Weibull fits of cases 1–3.

Case	Model	Parameter	RRMSE
1	Bohart-Adams	$\alpha = 1.901; \beta = 0.008 \text{ min}^{-1}$	0.081
	Weibull	$\alpha = 294.4 \text{ min}; b = 1.073$	0.032
2	Bohart-Adams	$\alpha = 8.288; \beta = 0.071 \text{ min}^{-1}$	0.029
	Weibull	$\alpha = 126.5 \text{ min}; b = 5.634$	0.032
3	Bohart-Adams	$\alpha = 4.522; \beta = 0.004 \text{ min}^{-1}$	0.032
	Weibull	$\alpha = 1416 \text{ min}; b = 2.875$	0.032

As shown in [Table 1](#), the estimated value of the b -term is 1.073, which translates to an inflection point located at $c/c_0 = 0.066$, according to Eq. (7). Because this location is close to the origin, the concave part of the Weibull fit is virtually nonvisible in [Fig. 1](#). The convex part dominates the overall shape of the predicted curve, making the Weibull fit look like a hyperbolic curve. The floating inflection point attribute allows the Weibull function to mimic the asymmetric shape of the data depicted in [Fig. 1](#) to a significant degree of precision.

In addition to its poor fit, [Fig. 1](#) reveals another serious shortcoming of the Bohart-Adams model: at $t = 0$, the predicted curve intersected the vertical axis at a nonzero c/c_0 value. This nonzero value may be estimated from the following equation:

$$\frac{c}{c_0} = \frac{1}{1 + \exp(\alpha)} \quad (8)$$

From [Table 1](#), $\alpha = 1.901$, and Eq. (8) yields $c/c_0 = 0.13$. This relatively large c/c_0 value contradicts the expected value of zero. Consequently, the Bohart-Adams model cannot be used to predict the breakthrough time corresponding to any effluent concentration level less than 13%.

To illustrate this limitation, we now use the Bohart-Adams model to compute the breakthrough time corresponding to an effluent concentration level of 10%. This breakthrough time may be estimated from the following rearranged form of the Bohart-Adams model:

$$t = \frac{1}{\beta} \left[\alpha - \ln\left(\frac{c_0}{c} - 1\right) \right] \quad (9)$$

Using the values of α and β given in [Table 1](#) and $c_0/c = 10$, Eq. (9) spits out a breakthrough time of -37 min. This negative breakthrough time is clearly nonsensical, and can have no physical significance whatsoever.

A rigorous version of the Bohart-Adams model, derived by [Amundson \(1948\)](#), is written as

$$\frac{c}{c_0} = \frac{\exp[\beta(t - \varepsilon L/u)]}{\exp(\alpha) + \exp[\beta(t - \varepsilon L/u)] - 1} \quad (10)$$

where ε is the bed voidage. Eq. (10) also produces a nonzero effluent concentration of 13% at time zero when it is fit to the breakthrough curve depicted in [Fig. 1](#) (assuming $\varepsilon = 0.4$). Likewise, it predicts a breakthrough time of -37 min at $c/c_0 = 10\%$. Evidently, this shortcoming is inherent in the simplified and rigorous forms of the Bohart-Adams model. It should be mentioned in passing that the recent work of [Hu and Zhang \(2020\)](#) presents an erroneous version of Eq. (10), as pointed out by [Chu \(2020b\)](#).

The Weibull function, by contrast, is well behaved at time zero. When $t = 0$, Eq. (1) predicts $c/c_0 = 0$. It also predicts a sensible breakthrough time corresponding to any predetermined effluent concentration level, which may be computed from the following equation:

$$t = \left[-\frac{1}{a} \ln\left(1 - \frac{c}{c_0}\right) \right]^{\frac{1}{b}} \quad (11)$$

Plugging the values of a and b given in [Table 1](#) and $c/c_0 = 0.1$ into Eq. (11) we get a breakthrough time of 40.2 min. This predicted breakthrough time is in fair agreement with the observed breakthrough time of 49.6 min corresponding to a similar breakthrough concentration of 9%. As mentioned earlier, the breakthrough time at 10% breakthrough predicted by the Bohart-Adams model is -37 min, which makes no sense.

In summary, the Weibull function is definitely superior to the Bohart-Adams model in representing the highly asymmetric breakthrough data depicted in [Fig. 1](#). Its three notable attributes are as follows: (1) excellent representation of highly asymmetric breakthrough data, (2) prediction of

zero effluent concentration at time zero, and (3) prediction of reliable breakthrough (and exhaustion) time corresponding to any predetermined effluent concentration level.

4.2. Case 2: Cr(III) adsorption by biomass

In this example, the plant *Agave lechuguilla* was used to remove Cr(III) from aqueous solutions (Romero-González et al., 2009). After washing, the leaves of the plant were oven dried and ground to pass through a 0.15 mm sieve. The dried biomass was packed in glass columns with an internal diameter of 0.7 cm. Column tests were carried out at 22 °C and pH 4 using different packed bed lengths and flow rates. The column test examined here was conducted with an initial Cr(III) concentration of 4 mg/L, a packed bed length of 10 cm, and a flow rate of 1 cm³/min.

Fig. 2 presents the observed breakthrough data and predicted curves of the Bohart-Adams and Weibull models for the selected column test. Fig. 2 shows that there is no immediate Cr(III) breakthrough in this case. Both models appear to fit the breakthrough profile very well; however, closer inspection of Fig. 2 reveals that the Bohart-Adams model tracks the curvature around the saturation region a bit better. This visual comparison is confirmed by the similar RRMSE scores, as presented in Table 1, case 2. The difference between the two RRMSE values is trivial.

The inflection point of the Weibull fit, computed from Eq. (7) using the estimated value of the *b*-term given in Table 1, is located at $c/c_0 = 0.56$. This location is close to the mid-point, revealing that the predicted Weibull curve is fairly symmetric.

One can see from Fig. 2 that the predicted curve of the Bohart-Adams model lies very close to the horizontal axis before the start of Cr(III) breakthrough, and there is no noticeable nonzero effluent concentration at time zero. The c/c_0 value at $t = 0$ predicted by the Bohart-Adams model from Eq. (8) is 0.0003, which is practically zero. When the Bohart-Adams model is used to fit highly symmetric breakthrough data, the problem of nonzero effluent concentration at time zero becomes much less conspicuous. As mentioned earlier, the Weibull function will always give an effluent concentration of zero at time zero.

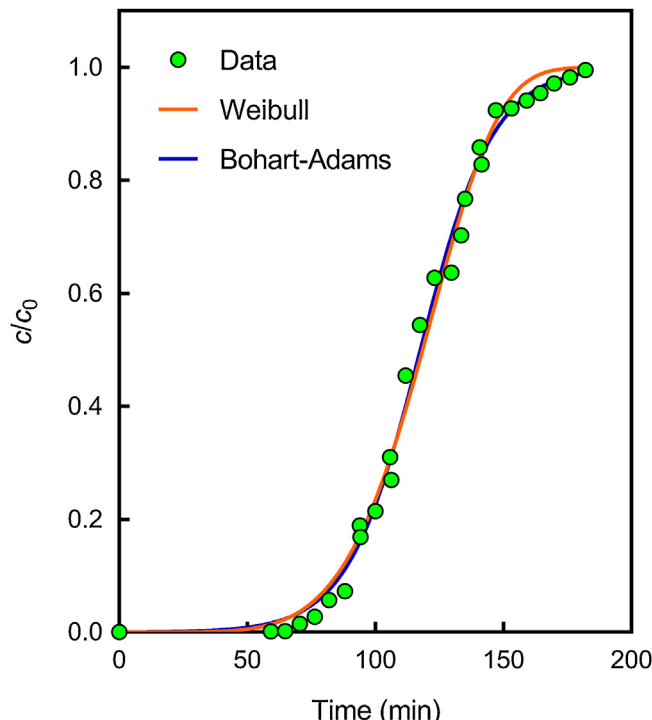


Fig. 2. Bohart-Adams and Weibull fits compared to observed Cr(III) breakthrough data reported by Romero-González et al. (2009).

If the breakthrough concentration is 10%, the breakthrough times predicted by the Bohart-Adams [Eq. (9)] and Weibull [Eq. (11)] equations are respectively 85.8 and 84.8 min. In this case, there is little difference between the two models with regard to overall fit and prediction of breakthrough time.

4.3. Case 3: Cr(VI) adsorption by coir pith

This case reports the removal of Cr(VI) from electroplating wastewater by coconut coir pith which was packed in two acrylic columns connected in series (Suksabye et al., 2008). Each column had an internal diameter of 5 cm and a length of 35 cm. A series of fixed bed experiments were conducted to investigate the effects of bed depth and flow rate. Because an actual electroplating wastewater stream containing Cr(VI) was used for testing, the feed concentration was the same for all fixed bed experiments.

Fig. 3 presents the observed breakthrough curve of the selected data set, obtained with a very large feed concentration of 1532 mg/L, a bed depth of 40 cm, and a flow rate of 10 cm³/min. The observed breakthrough curve is moderately asymmetric, displaying an apparent leakage of Cr(VI) during the early stages of the fixed bed test. Also shown in Fig. 3 are the predicted curves of the Bohart-Adams and Weibull models. The associated parameter estimates and RRMSE values are presented in Table 1, case 3. The two model fits are clearly visually similar, and the associated RRMSE values support this. The shapes of the two fits are so similar that it is difficult to discern the lines. However, closer inspection of Fig. 3 reveals that the Weibull function has a better ability to model the initial stages of the breakthrough profile than the Bohart-Adams model.

The inflection point of the Weibull curve, computed from Eq. (7) with the estimated value of the *b*-term given in Table 1, is located at $c/c_0 = 0.48$. This location is very close to the mid-point, indicating that the predicted Weibull curve is highly symmetric. It is thus not surprising to see that the Weibull fit is very similar to the Bohart-Adams fit, the inflection point of which is located at the mid-point.

However, there are noticeable deviations between the fits and observed data in the initial and later stages. These deviations will affect

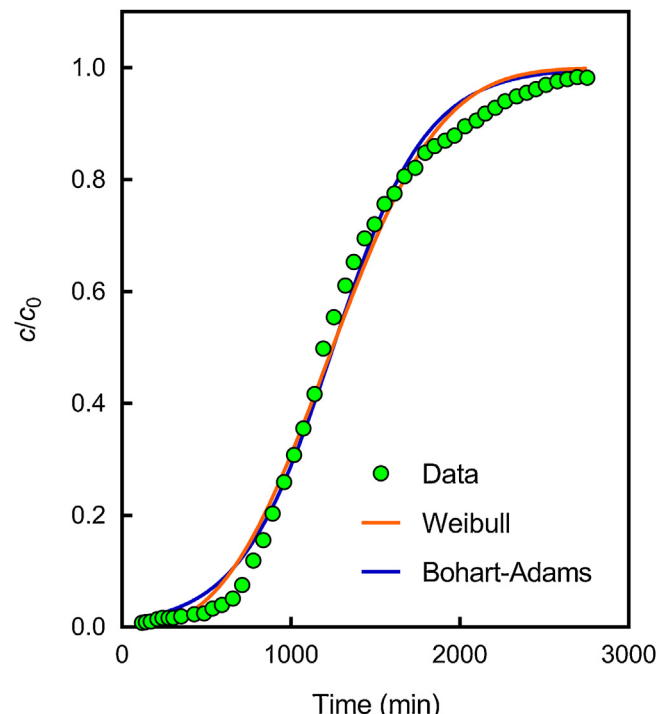


Fig. 3. Bohart-Adams and Weibull fits compared to observed Cr(VI) breakthrough data reported by Suksabye et al. (2008).

the ability of the two models to provide reliable estimates of breakthrough and exhaustion times. Given its excellent ability to correlate the highly asymmetric breakthrough data of case 1, it is somewhat surprising to note that the performance of the Weibull function is not much better than that of the Bohart-Adams model in representing the Fig. 3 profile, which seems to exhibit a moderate degree of curve asymmetry. It appears that such breakthrough data could pose a formidable challenge to the Weibull function. Although the Weibull function has a floating inflection point, its functional form is probably not flexible enough to allow it to represent a wide range of breakthrough data exhibiting different degrees of curve asymmetry.

5. Conclusions

- The Weibull function is very effective in tracking the shape of the highly asymmetric breakthrough data of Cr(III) adsorption in a fixed bed adsorber packed with olive stone particles. The performance of the Bohart-Adams model is very poor because its inflexible functional form restricts its ability to describe such data.
- When challenged with the breakthrough data of Cr(VI) adsorption in a fixed bed column packed with coir pith, the performance of the Weibull function is fair and similar to that of the Bohart-Adams model.
- Both models can describe the slightly asymmetric breakthrough data of Cr(III) adsorption in a fixed bed column packed with a biosorbent.
- The Weibull function is devoid of typical fixed bed variables. As a result, it cannot be used for process design. Work is underway to link its two empirical parameters to important fixed bed variables (e.g., feed concentration, flow rate, and bed length) and the results will be reported in a future communication.

Funding

The author received no specific funding for writing this article.

Declaration of competing interest

The author declares he has no competing interest.

References

Altenor, S., Carene, B., Emmanuel, E., Lambert, J., Ehrhardt, J.-J., Gaspard, S., 2009. Adsorption studies of methylene blue and phenol onto vetiver roots activated carbon prepared by chemical activation. *J. Hazard. Mater.* 165, 1029–1039.

Amundson, N.R., 1948. A note on the mathematics of adsorption in beds. *J. Phys. Colloid Chem.* 52, 1153–1157.

Apiratikul, R., Chu, K.H., 2021. Improved fixed bed models for correlating asymmetric adsorption breakthrough curves. *J. Water Process Eng.* 40101810.

Avrami, M., 1940. Kinetics of phase change. II. Transformation-time relations for random distribution of nuclei. *J. Chem. Phys.* 8, 212–224.

Bohart, G.S., Adams, E.Q., 1920. Some aspects of the behavior of charcoal with respect to chlorine. *J. Am. Chem. Soc.* 42, 523–544.

Calero, M., Hernández, F., Blázquez, G., Tenorio, G., Martín-Lara, M.A., 2009. Study of Cr (III) biosorption in a fixed-bed column. *J. Hazard. Mater.* 171, 886–893.

Chatterjee, A., Schiewer, S., 2011. Biosorption of cadmium(II) ions by citrus peels in a packed bed column: effect of process parameters and comparison of different breakthrough curve models. *Clean-Soil Air Water* 39, 874–881.

Chen, S.G., Yang, R.T., 1994. Theoretical basis for the potential theory adsorption isotherms. The Dubinin-Radushkevich and Dubinin-Astakhov equations. *Langmuir* 10, 4244–4249.

Chu, K.H., 2020a. Fitting the Gompertz equation to asymmetric breakthrough curves. *J. Environ. Chem. Eng.* 8, 103713.

Chu, K.H., 2020b. Rebuttal to comment on “Breakthrough curve analysis by simplistic models of fixed bed adsorption: in defense of the century-old Bohart-Adams model”. *Chem. Eng. J.* 398, 125546.

Dima, J.B., Ferrari, M., Zaritsky, N., 2020. Mathematical modeling of fixed-bed columns adsorption: hexavalent chromium onto chitosan flakes. *Ind. Eng. Chem. Res.* 59, 15378–15386.

GracePavithra, K., Jaikumar, V., Kumar, P.S., SundarRajan, P., 2019. A review on cleaner strategies for chromium industrial wastewater: present research and future perspective. *J. Clean. Prod.* 228, 580–593.

Guiza, S., Brouers, F., Bagane, M., 2021. Fluoride removal from aqueous solution by montmorillonite clay: kinetics and equilibrium modeling using new generalized fractal equation. *Environ. Technol. Innov.* 21, 101187.

Hu, Q., Zhang, Z., 2020. Comment on “Breakthrough curve analysis by simplistic models of fixed bed adsorption: in defense of the century-old Bohart-Adams model”. *Chem. Eng. J.* 394 (2020) 124511.

Hutchins, R.A., 1973. New method simplifies design of activated carbon systems. *Chem. Eng.* 80, 133–138.

Hutson, N.D., Yang, R.T., 1997. Theoretical basis for the Dubinin-Radushkevitch (DR) adsorption isotherm equation. *Adsorption* 3, 189–195.

Kinniburgh, D.G., 1986. General purpose adsorption isotherms. *Environ. Sci. Technol.* 20, 895–904.

Lee, C.-G., Kim, J.-H., Kang, J.-K., Kim, S.-B., Park, S.-J., Lee, S.-H., Choi, J.-W., 2015. Comparative analysis of fixed-bed sorption models using phosphate breakthrough curves in slag filter media. *Desalin. Water Treat.* 55, 1795–1805.

Marangoni, A.G., 1998. On the use and misuse of the Avrami equation in characterization of the kinetics of fat crystallization. *J. Am. Oil Chem. Soc.* 75, 1465–1467.

Ncibi, M.C., Altenor, S., Seffen, M., Brouers, F., Gaspard, S., 2008. Modelling single compound adsorption onto porous and non-porous sorbents using a deformed Weibull exponential isotherm. *Chem. Eng. J.* 145, 196–202.

Njoku, V.O., Asif, M., Hameed, B.H., 2015. 2,4-Dichlorophenoxyacetic acid adsorption onto coconut shell-activated carbon: isotherm and kinetic modeling. *Desalin. Water Treat.* 55, 132–141.

Oladoja, N.A., 2016. A critical review of the applicability of Avrami fractional kinetic equation in adsorption-based water treatment studies. *Desalin. Water Treat.* 57, 15813–15825.

Oulman, C.S., 1980. The logistic curve as a model for carbon bed design. *J. Am. Water Works Assn.* 72, 50–53.

Peng, H., Guo, J., 2020. Removal of chromium from wastewater by membrane filtration, chemical precipitation, ion exchange, adsorption electrocoagulation, electrochemical reduction, electrodialysis, electrodeionization, photocatalysis and nanotechnology: a review. *Environ. Chem. Lett.* 18, 2055–2068.

Romero-González, J., Walton, J.C., Peralta-Videa, J.R., Rodríguez, E., Romero, J., Gardea-Torresdey, J.L., 2009. Modeling the adsorption of Cr(III) from aqueous solution onto *Agave lechugilla* biomass: study of the advective and dispersive transport. *J. Hazard. Mater.* 161, 360–365.

Selmi, T., Seffen, M., Sammouda, H., Mathieu, S., Jagiello, J., Celzard, A., Fierro, V., 2018. Physical meaning of the parameters used in fractal kinetic and generalised adsorption models of Brouers-Sotolongo. *Adsorption* 24, 11–27.

Suksabye, P., Thiravetyan, P., Nakbanpote, W., 2008. Column study of chromium(VI) adsorption from electroplating industry by coconut coir pith. *J. Hazard. Mater.* 160, 56–62.

Weibull, W., 1951. A statistical distribution function of wide applicability. *J. Appl. Mech.* 18, 293–297.